Available online at www.sciencedirect.com
ScienceDirect
Journal of Sound and Vibration 299 (2007) 339–347
JOURNAL OF SOUND AND VIBRATION
www.elsevier.com/locate/jsvi

Short Communication

External and internal coupling effects of rotor's bending and torsional vibrations under unbalances

Zhenwei Yuan[a,b,*], Fulei Chu[a], Yanli Lin[a]

[a]*Department of Precision Instruments and Mechanology, Tsinghua University, Beijing 100084, China*
[b]*School of Chemical Engineering, Zhengzhou University, Zhengzhou 450002, China*

Received 29 November 2005; received in revised form 25 April 2006; accepted 23 June 2006
Available online 11 September 2006

Abstract

External and internal bending–torsion coupling effects of a rotor system with comprehensive unbalances are studied by analytical analysis and numerical simulations. Based on Lagrangian approach, a full-degree-of-freedom dynamic model of a Jeffcott rotor is developed. The harmonic balance method and the Floquet theory are combined to analyze the stability of the system equations. Numerical simulations are conducted to observe the bending–torsion coupling effects. In the formulation of rotordynamic model, two bending–torsion coupling patterns, external coupling and internal coupling, are suggested. By analytical analysis, it is concluded that the periodic solution of the system is asymptotically stable. From numerical simulations, three bending–torsion coupling effects are observed in three cases. Under static unbalance, synchronous torsional response is observed, which is the result of external coupling under unbalanced force. Under dynamic unbalance, two-time synchronous frequency torsional response is observed, which is the result of internal coupling under unbalanced moment. Under comprehensive unbalance, synchronous and two-time synchronous frequency torsional components are observed, which are the results of both external and internal couplings under unbalanced force and moment. These observations agree with the analytical analysis. It is believed that these observed phenomena should make sense in the dynamical design and fault diagnostics of a rotor system.

1. Introduction

Rotor's vibration is a complicated kinetical and dynamical phenomenon. It seriously affects the normal operation of a system and even leads to catastrophic consequences. So far, large amount of research work has been done and great progresses have been made for the problem. With the development of high performance turbomachinery, it becomes a great challenge to researchers in that the problem gets more and more complicated with the more and more sophisticated system on one hand, the requirement for stability and reliability grows higher and higher on the other. Therefore, it is required that the rotordynamic model of a system account for all the factors that could affect the dynamic behaviors of the system. Among them is bending–torsion coupling in the vibration of a rotor system.

*Corresponding author. Department of Precision Instruments and Mechanology, Tsinghua University, Beijing 100084, China. Tel.: +86 10 62772095.
E-mail address: yuanzw02@mails.tsinghua.edu.cn (Z. Yuan).

0022-460X/$ - see front matter © 2006 Elsevier Ltd. All rights reserved.
doi:10.1016/j.jsv.2006.06.054

For bending–torsion coupling, researches have been done in many aspects. In rotordynamic modeling, Mohiuddin and Khulief [1] derived an elastodynamic model of coupled bending and torsional system using the Lagrangian approach. The model accounted for the gyroscopic effects as well as the inertia coupling between bending and torsional deformations and therefore provided an efficient tool for dynamic analysis of rotor-bearing systems. Liu et al. [2] constructed the nonlinear dynamic model of a rotor with coupled bending and torsional vibrations and studied the nonlinear dynamic characteristics of the rotor. In dynamics of unbalanced rotor systems, Huang et al. [3] derived a rotordynamic model of a Jeffcott rotor under unbalance that accounted for bending–torsion coupling, with the consideration of three degrees of freedom (dofs), including two lateral displacements and a torsional angle, and obtained the dynamic characteristics of the unbalanced rotor with bending–torsion coupling by solving the nonlinear differential equations using Wilson-θ method. In dynamics of rotor's rub-impacts, Al-Bedoor [4] presented a model for the coupled torsional and lateral vibrations of unbalanced rotors with rotor-to-stator rubbing using Lagrangian dynamics. The model accounted for the rotor rigid-body rotation, the rotor torsional deformation and two orthogonal lateral deflections of the rotor. It was pointed out that the inclusion of rotor torsional flexibility had introduced irregular rubbing orbits. And also, a split in resonance was observed due to the rubbing condition when the rotor torsional flexibility was considered. Sun et al. [5] established a mathematical model of an impacting-rub rotor system with bending–torsion coupling and discussed the influence of bending–torsion coupling on the dynamic characteristics of an impacting-rub rotor system by a comparison with the model without bending–torsion coupling. In dynamics of cracked rotors, Xiao and Yang [6] investigated the bending–torsional coupled vibration of a level Jeffcott rotor containing a switching transverse crack. It was concluded that torsional vibration could greatly influence the dynamic behaviors of a rotor with switching transverse cracks. Zhao et al. [7] researched the bending–torsion coupling characteristics of cracked rotors and analyzed the influences of torsional vibration on lateral vibration. It was pointed out that the bending–torsion coupling effects could undermine the dynamic characteristics of cracked rotor. Zhu and Zhao [8] studied the coupled vibration of a cracked rotor. In dynamics of rotor and blade, de Goeij et al. [9] investigated the implementation of bending–torsion coupling of a composite wind turbine rotor blade to provide passive pitch-control. Al-Bedoor [10] developed a dynamic model of coupled shaft torsional and blade bending deformations in rotors. The model accounted for all the dynamic coupling terms between the system reference rotational motion, shaft torsional deformations and blade bending deformations.

In this paper, the bending–torsion coupling effects are investigated with differences in two ways from previous researches. The rotordynamic model is established in all the six dofs of a rotor other than in three or four dofs as in previous researches. On the other hand, comprehensive unbalances including static unbalance and dynamic unbalance as excitations are involved in the model instead of only involving static unbalance as suggested in previous literatures.

2. Dynamic model

2.1. Basic definitions and assumptions

The system dynamic model is developed based on a Jeffcott rotor with the following assumptions: (1) the model adopts the simple Jeffcott approach that considers the system as a rigid disk mounted midway between the two supports on a massless flexible shaft; (2) the system has proportional damping, i.e., the system damping is proportional to velocity; (3) only the unbalances are considered as external excitations; (4) gyroscopic effects is taken into account; and (5) all the six dofs of the disk are involved.

In Fig. 1, $oxyz$ is a fixed coordinate system. $o'\xi\eta\zeta$ is a rotating coordinate system with the rotor. o is the center of the static rotor. o' is the center of the running rotor. E is the mass center of the rotor. me is the quantity of mass unbalance. The $oxyz$ and $o'\xi\eta\zeta$ are identical when the rotor is at rest. Assume that the generalized coordinate vector of the rotor is $\{\mathbf{q}\} = [x \quad \theta_y \quad y \quad \theta_x \quad z \quad \theta_z]^{\mathrm{T}}$, where x, y and z are the displacements of the disk center in x, y and z directions, respectively, θ_x and θ_y are the pitching angles of the disk around axes x and y, respectively, θ_z is the torsional angle (caused by torsional deformation) of the shaft around axis z at the disk center. The equation of motions of the rotor is developed as follows.

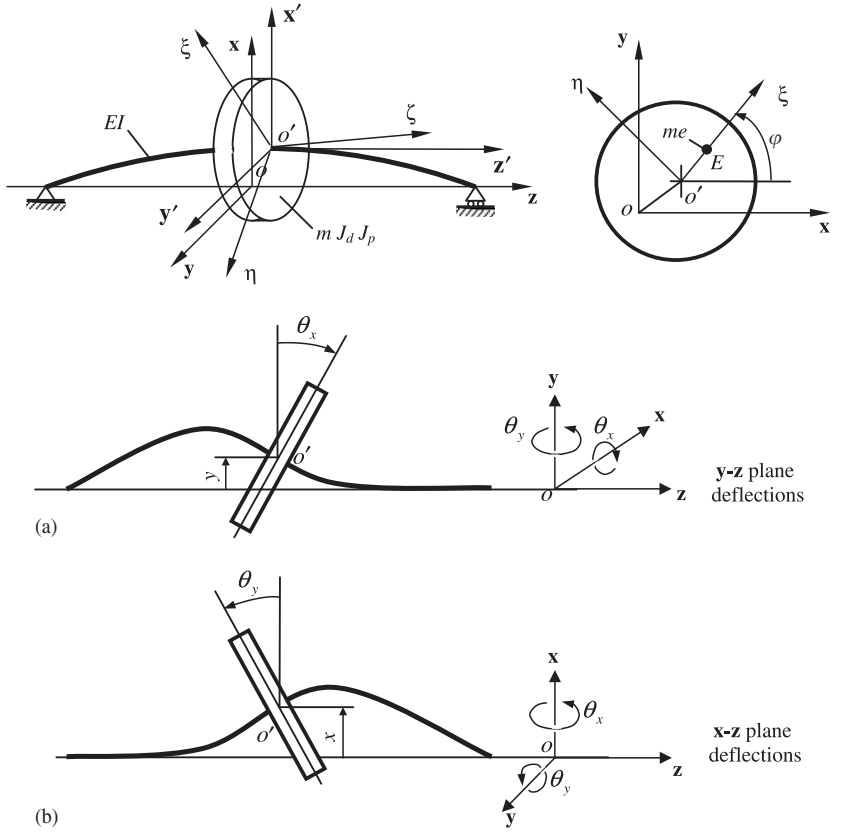

Fig. 1. Definitions of coordinate systems and variables.

2.2. Derivation of system equations of motion

The kinetic energy of the rotor can be defined by

$$T = \frac{1}{2}m\left(\dot{x}^2 + \dot{y}^2 + \dot{z}^2\right) + \frac{1}{2}\left[J_d\dot{\theta}_x^2 + J_d\dot{\theta}_y^2 + J_p\left(\dot{\theta}_z + \Omega\right)^2 - 2J_p\theta_x\dot{\theta}_y\left(\dot{\theta}_z + \Omega\right)\right], \tag{1}$$

where m is the mass of the rotor, J_d and J_p are the diameter and polar inertia moments of the rotor disk respectively, Ω is the rotating angular velocity of the rotor.

The elastic potential energy of the system is defined as

$$V = \frac{1}{2}\left(k_x x^2 + k_{\theta y}\theta_y^2 + k_y y^2 + k_{\theta x}\theta_x^2 + k_z z^2 + k_{\theta z}\theta_z^2\right), \tag{2}$$

where k_x, k_y and k_z are the stiffness coefficients corresponding to x, y and z, respectively, $k_{\theta x}$, $k_{\theta y}$ and $k_{\theta z}$ are the stiffness coefficients corresponding to θ_x, θ_y and θ_z, respectively.

Using the Lagrangian approach, the equations of motion of the system are derived as

$$[\mathbf{M}]\{\ddot{q}\} + [\mathbf{C}]\{\dot{q}\} + [\mathbf{K}]\{q\} = \{\mathbf{Q}\}, \tag{3}$$

where $\{\mathbf{Q}\} = \{\mathbf{Q}_c\} + \{\mathbf{Q}_u\}$ is the generalized force vector; $\{\mathbf{Q}_c\} = [0 \quad M_{cy} \quad 0 \quad M_{cx} \quad 0 \quad M_{cz}]^{\mathrm{T}}$ is the internal coupling force vector, which will be defined in Section 2.3; $\{\mathbf{Q}_u\} = [F_{ux} \quad M_{uy} \quad F_{uy} \quad M_{ux} \quad 0 \quad M_{uz}]^{\mathrm{T}}$ is the external coupling unbalanced force vector, which includes static and dynamic unbalanced forces and will be

defined in Section 2.4; $[\mathbf{M}] = \mathrm{diag}(m, J_d, m, J_d, m, J_p)$ is the inertia matrix;

$$[\mathbf{C}] = \begin{bmatrix} c_x & 0 & 0 & 0 & 0 & 0 \\ 0 & c_{\theta y} & 0 & \Omega J_p & 0 & 0 \\ 0 & 0 & c_y & 0 & 0 & 0 \\ 0 & -\Omega J_p & 0 & c_{\theta x} & 0 & 0 \\ 0 & 0 & 0 & 0 & c_z & 0 \\ 0 & 0 & 0 & 0 & 0 & c_{\theta z} \end{bmatrix}$$

is the damping matrix with the gyroscopic effects embedded in it; $[\mathbf{K}] = \mathrm{diag}\left(k_x, k_{\theta y}, k_y, k_{\theta x}, k_z, k_{\theta z}\right)$ is the stiffness matrix. The other elements except for the gyroscopic term ΩJ_p in $[\mathbf{C}]$ are determined by experience. The elements in $[\mathbf{K}]$ are calculated by static analysis with influence coefficient method, with the shaft being regarded as a simply supported beam.

2.3. Definition of internal coupling forces

From the formulation of Eq. (3), the nonlinear internal coupling forces can be defined as

$$\begin{aligned} M_{cx} &= -J_p \dot{\theta}_y \dot{\theta}_z, \\ M_{cy} &= J_p\left(\dot{\theta}_x \dot{\theta}_z + \theta_x \ddot{\theta}_z\right), \\ M_{cz} &= J_p\left(\dot{\theta}_x \dot{\theta}_y + \theta_x \ddot{\theta}_y\right). \end{aligned} \tag{4}$$

2.4. Development of external coupling forces

Through kinetical analysis and by using Dalembert principle, the external coupled unbalanced forces can be stated as

$$\begin{aligned} F_{ux} &= me_1\left[\left(\Omega + \dot{\theta}_z\right)^2 \cos\left(\Omega t + \theta_z + \phi_1\right) + \ddot{\theta}_z \sin\left(\Omega t + \theta_z + \phi_1\right)\right], \\ F_{uy} &= me_1\left[\left(\Omega + \dot{\theta}_z\right)^2 \sin\left(\Omega t + \theta_z + \phi_1\right) - \ddot{\theta}_z \cos\left(\Omega t + \theta_z + \phi_1\right)\right], \\ F_{uz} &= 0, \\ M_{ux} &= me_2 h\left[\left(\Omega + \dot{\theta}_z\right)^2 \sin\left(\Omega t + \theta_z + \phi_2\right) - \ddot{\theta}_z \cos\left(\Omega t + \theta_z + \phi_2\right)\right], \\ M_{uy} &= -me_2 h\left[\left(\Omega + \dot{\theta}_z\right)^2 \cos\left(\Omega t + \theta_z + \phi_2\right) + \ddot{\theta}_z \sin\left(\Omega t + \theta_z + \phi_2\right)\right], \\ M_{uz} &= me_1\left[\ddot{x}\sin\left(\Omega t + \theta_z + \phi_1\right) - (\ddot{y} + g)\cos\left(\Omega t + \theta_z + \phi_1\right)\right]. \end{aligned} \tag{5}$$

3. Analytical analysis

The above developed dynamic model is nonlinear. The harmonic balance method and the Floquet theory are combined to give qualitative analysis of the stability of the system. First, a stable periodic solution of the system equation is obtained with the harmonic balance method. Then, the equation is perturbed at the obtained solution to get the perturbation equation. Finally, the zero solution stability of the perturbation equation is analyzed with the Floquet theory, and accordingly the periodic solution stability of the system is determined. It is concluded that: (1) when the system is subject to static unbalance, there is sole synchronous vibration in x, y and θ_z; (2) when the system is subject to dynamic unbalance, there is sloe synchronous vibration in θ_x and θ_y and there is sole two-time synchronous frequency vibration in θ_z; (3) when the system is subject to comprehensive unbalance, there is sole synchronous vibration in x, y, θ_x and θ_y, but there are both synchronous and two-time synchronous frequency vibrations in θ_z.

Table 1 lists the characteristic multipliers $\lambda_i < 1 (i = 1, 2, \ldots, 10)$ of the perturbation equation at different rotating speeds. Fig. 2 gives an overview of the characteristic multipliers in the range of $\Omega/\Omega_0 = 0.6692 \sim 10$, where Ω is rotating frequency, $\Omega_0 = \sqrt{k_{\theta z}/J_p}$.

In the light of Floquet theory, when $|\lambda_i| < 1$ $(i = 1, 2, \ldots, n)$, the solution of the system is asymptotically stable; if one or more than one of $|\lambda_i| < 1$ $(i = 1, 2, \ldots, n)$ is/are beyond one, the solution of the system is unstable; if one or more than one of $|\lambda_i| < 1$ $(i = 1, 2, \ldots, n)$ equal(s) to one, the solution of the system is critical.

From Table 1, it can be seen that the moduli of all the listed characteristic multipliers are less than one. This indicates that the zero solution of the perturbation equation is asymptotically stable at the corresponding rotating speeds. From Fig. 2 it can be clearly observed that the moduli of the characteristic multipliers are roofed by the unit line in the full range of rotating speed and never touch the roof line. Therefore, it could be concluded that the zero solution of the perturbation equation is asymptotically stable for all speeds. This means that the solution of the system equation is asymptotically stable.

Table 1
Characteristics of bending–torsion couplings at different rotating speeds

Ω/Ω_0	0.6692	2.0	4.0	6.0	8.0	10.0
λ_1	$-0.3812+0.0318i$	$-0.7258+0.0203i$	$0.0119+0.8520i$	$0.4566+0.7741i$	$0.6572+0.6481i$	$0.7618+0.5471i$
λ_2	$-0.3812-0.0318i$	$-0.7258-0.0203i$	$0.0119-0.8520i$	$0.4566-0.7741i$	$0.6572-0.6481i$	$0.7618-0.5471i$
λ_3	0.2578	0.6365	0.7978	0.8602	0.8932	0.9136
λ_4	0.2578	0.6365	0.7978	0.8602	0.8932	0.9136
λ_5	0	0.0288	0.1697	0.3065	0.4120	0.4920
λ_6	0	0.0288	0.1697	0.3065	0.4120	0.4920
λ_7	0	$0.0192+0.0043i$	$-0.2126+0.2805i$	$0.2700+0.6043i$	$0.6272+0.5268i$	$0.8000+0.4022i$
λ_8	0	$0.0192-0.0043i$	$-0.2126-0.2805i$	$0.2700-0.6043i$	$0.6272-0.5268i$	$0.8000-0.4022i$
λ_9	0	0	$-0.0006+0.0008i$	$0.0030+0.0066i$	$0.0171+0.0143i$	$0.0406+0.0204i$
λ_{10}	0	0	$-0.0006-0.0008i$	$0.0030-0.0066i$	$0.0171-0.0143i$	$0.0406-0.0204i$
	Asymptotically stable	Asymptotically stable	Asymptotically stable	Asymptotically stable	Asymptotically stable	Asymptotically stable

Notes: The axial vibration equation in Eq. (3) is removed in the analytical analysis to reduce the problem, for it does not couple with the other five equations and does not affect the analysis results. Therefore, only 10 characteristic multipliers are obtained.

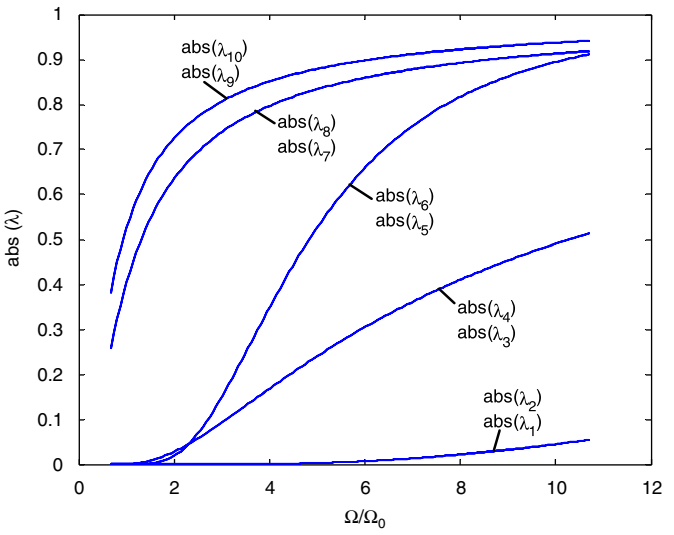

Fig. 2. Overview of $|\lambda_i|$ in a large range of rotating speed.

4. Numerical simulations

Since Eq. (3) is a set of nonlinear differential equations, the ODE solver *ode*45 in MATLAB is used for numerical calculations. Three cases of unbalance, static, dynamic and comprehensive (the combination of the former two), are considered here. Parameters related to the calculations are listed in Table 2.

5. Bending–torsion coupling effects

Figs. 3–8 demonstrate the bending–torsion coupling effects represented in torsional response in three cases. They are the bending–torsion coupling effects under static unbalance, dynamic unbalance and comprehensive unbalance, respectively.

5.1. Bending– torsion coupling effects under static unbalance

Fig. 3 displays the waveform and frequency spectrum of torsional response under static unbalance. Evidently, a perfect synchronous torsional response is observed in the waveform and spectrum. It represents the external bending–torsion coupling effect of the system under static unbalance, which is indicated by Eq. (5). Fig. 4 is an overview of the coupling effects under static unbalance in a large range of rotating speed. It is clearly shown that the sole synchronous torsional response appears in a large range of rotating speed. This agrees with the analytical analysis.

Table 2
Parameters of the system

Parameters of the rotor	
Mass of the rotor disk, m, kg	2
Diameter of the rotor disk, D, m	0.1
Mass eccentricity of the static rotor disk unbalance, e_1, m	1×10^{-4}
Static phase angle of the static rotor disk unbalance, φ_1, rad	$\pi/3$
Mass eccentricity of the dynamic rotor disk unbalance, e_2, m	3×10^{-3}
Static phase angle of the dynamic rotor disk unbalance, φ_2, rad	$\pi/3$
Arm length of the dynamic rotor disk unbalance, h, m	0.005
Parameters of the shaft	
Diameter of the shaft, d, m	0.015
Total length of the shaft, L, m	0.5
Bending elastic modulus of the shaft, E, pa	2.1×10^{11}
Shearing elastic modulus of the shaft, G, pa	7.7×10^{10}

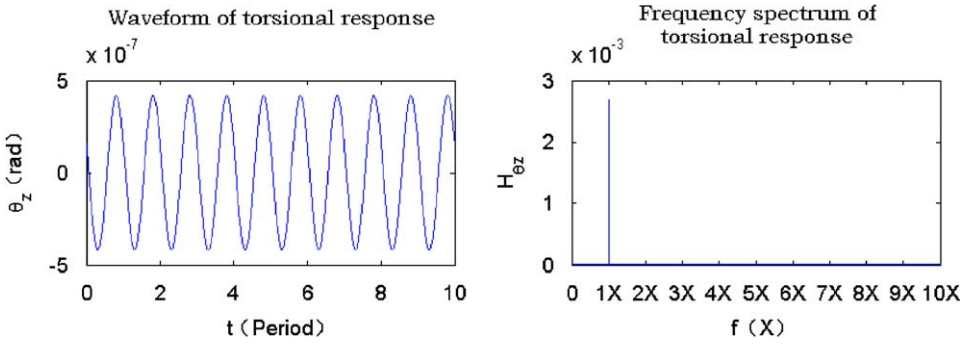

Fig. 3. Bending–torsion coupling effects under static unbalance at 15,000 rpm.

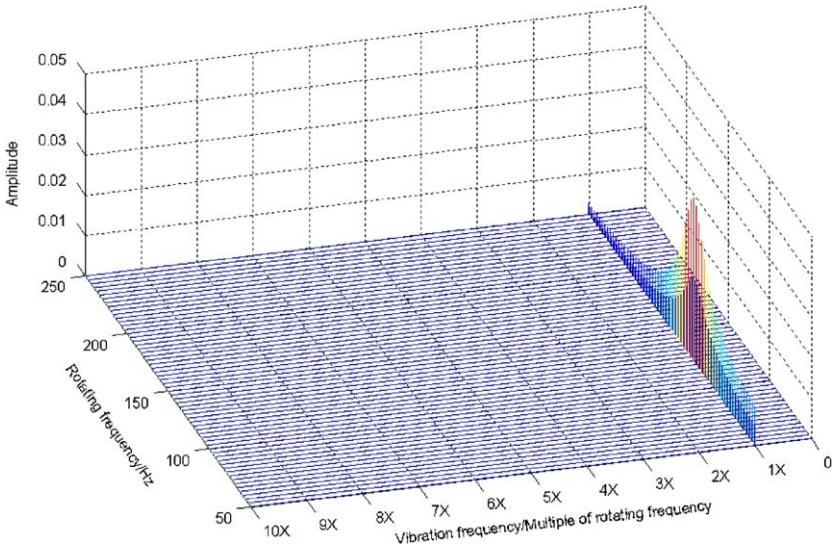

Fig. 4. Overview of the bending–torsion coupling effects under static unbalance.

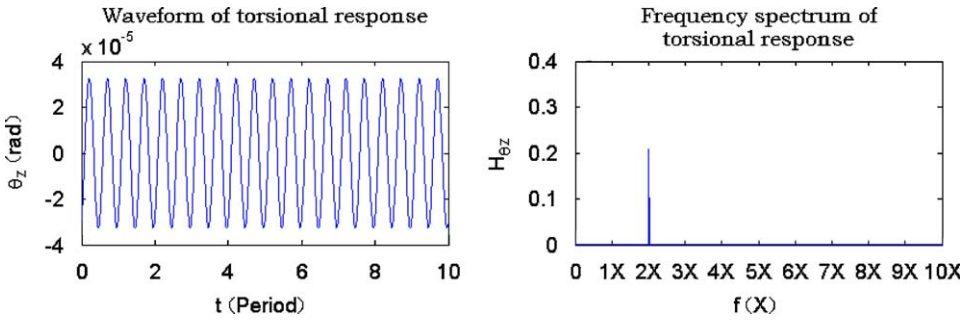

Fig. 5. Bending–torsion coupling effects under dynamic unbalance at 15,000 rpm.

5.2. Bending–torsion coupling effects under dynamic unbalance

Fig. 5 displays the waveform and frequency spectrum of torsional response under dynamic unbalance. Evidently, a perfect two-time synchronous frequency torsional response is observed in the waveform and spectrum. It represents the internal bending–torsion coupling effect of the system under dynamic unbalance, which is indicated by Eq. (4). Fig. 6 is an overview of the coupling effects under dynamic unbalance in a large range of rotating speed. It is clearly shown that the sole two-time synchronous frequency torsional response appears in a large range of rotating speed. This also agrees with the analytical analysis.

5.3. Bending–torsion coupling effects under comprehensive unbalance

Fig. 7 displays the waveform and frequency spectrum of torsional response under comprehensive unbalance. Evidently, a perfect synchronous component and a perfect two-time synchronous frequency component are observed in the waveform and spectrum of torsional response. They represent the comprehensive bending–torsion coupling effects of the system under comprehensive unbalance, which are the total results of external and internal couplings represented, respectively, by Eqs. (4) and (5). The synchronous component is caused by external coupling with static unbalance, and the two-time synchronous frequency component is caused by internal coupling with dynamic unbalance. Fig. 8 is an overview of the coupling effects under comprehensive unbalance in a large range of rotating speed. It is clearly shown that the

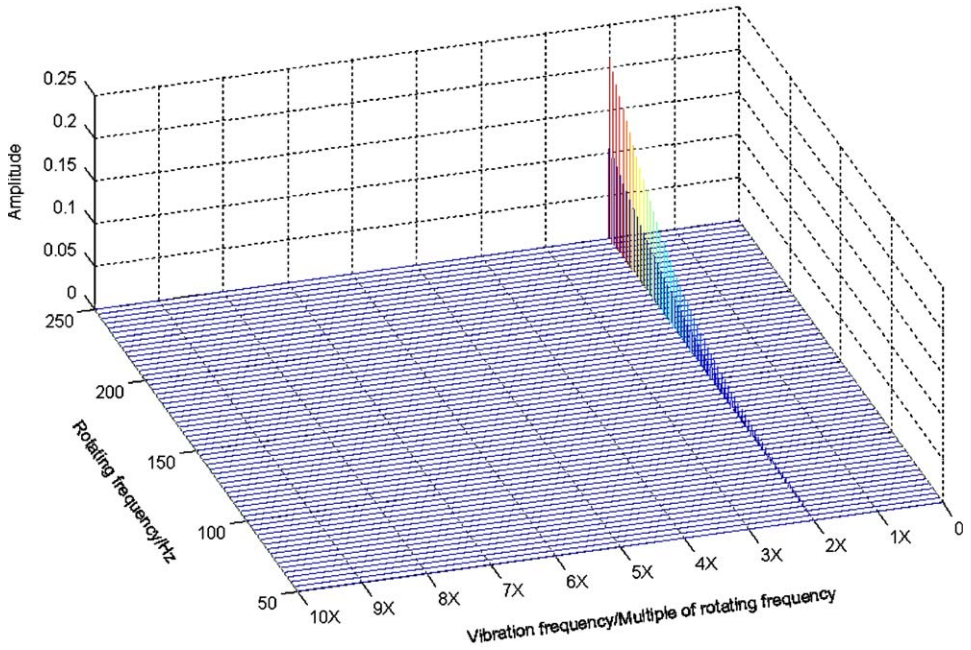

Fig. 6. Overview of the bending–torsion coupling effects under dynamic unbalance.

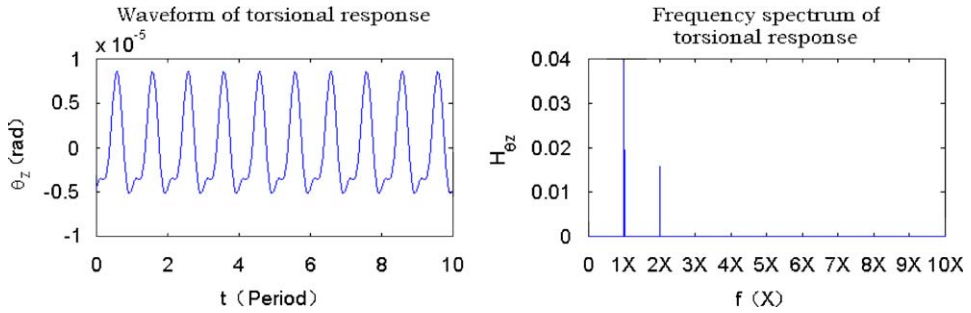

Fig. 7. Bending–torsion coupling effects under comprehensive unbalance at 15,000 rpm.

synchronous and two-time synchronous frequency components appear in a large range of rotating speed. This also agrees with the analytical analysis.

6. Conclusions

Through dynamic modeling, analytical analysis and numerical simulations, the internal and external bending–torsion coupling effects of a Jeffcott rotor with unbalances are studied with the following conclusions:

(1) Two bending–torsion coupling patterns, internal coupling and external coupling, are suggested in the present rotordynamic model from theoretical formulation.
(2) Analytical analysis verifies that the system equations have asymptotically stable periodic solution and justifies the numerical simulation results.
(3) Three bending–torsion coupling effects are observed from numerical simulations. Under static unbalance, sole synchronous torsional response is observed, which is the result of external coupling under unbalanced force. Under dynamic unbalance, sole two-time synchronous frequency torsional response is observed, which is the result of internal coupling under unbalanced moment. Under comprehensive unbalance,

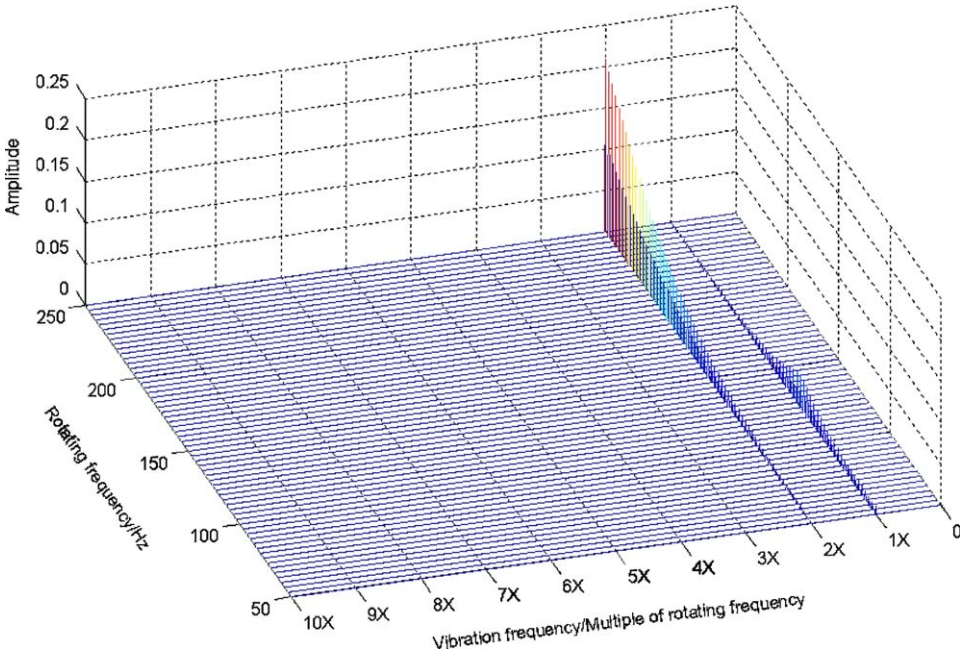

Fig. 8. Overview of the bending–torsion coupling effects under comprehensive unbalance.

a synchronous and a two-time synchronous frequency torsional components are observed, which are the total results of both external and internal couplings under unbalanced force and moment. These results agree with analytical analysis. It is believed that these observed phenomena should make sense in the dynamical design and fault diagnostics of a rotor system.

Acknowledgments

This research is supported by Natural Science Foundation of China (Grant no. 50425516) and the Trans-Century Training Programme Foundation for the Talents by the Ministry of Education.

References

[1] M.A. Mohiuddin, Y.A. Khulief, Coupled bending torsional vibration of rotors using finite element, *Journal of Sound and Vibration* 223 (2) (1999) 297–316.
[2] Z. Liu, Y. Cui, W. Huang, et al., Study of nonlinear dynamic characteristics of a rotor with coupled bending and torsional vibrations, *China Mechanical Engineering* 14 (7) (2003) 603–605.
[3] D.-G. Huang, L. Zhu, Z.-K. Jiang, Numerical simulation of unbalanced rotor with bending–torsion coupling, *Steam Turbine Technology* 37 (6) (1995) 346–348.
[4] B.O. Al-Bedoor, Transient torsional and lateral vibrations of unbalanced rotors with rotor-to-stator rubbing, *Journal of Sound and Vibration* 229 (3) (2000) 627–645.
[5] Z.-C. Sun, J.-X. Xu, et al., Study on influence of bending–torsion coupling in an impacting-rub rotor system, *Applied Mathematics and Mechanics* 24 (11) (2003) 1316–1323.
[6] X. Xiao, Z. Yang, G. Xiao, Study on bending–torsional coupled vibration of a rotor with a switching crack, *Acta Mechanica Solida Sinica* 24 (3) (2003) 334–340.
[7] Y. Zhao, S. Li, Q. Xu, Analysis on bending–torsional coupled vibration of cracked rotor, *Chinese Journal of Applied Mechanics* 16 (1) (1999) 60–64.
[8] H. Zhu, M. Zhao, A study on the coupled vibration of a cracked rotor, *Journal of Vibration Engineering* 14 (3) (2001) 349–353.
[9] W.C. de Goeij, M.J.L. van Tooren, A. Beukers, Implementation of bending–torsion coupling in the design of a wind-turbine rotor-blade, *Applied Energy* 63 (1999) 191–207.
[10] B.O. Al-Bedoor, Dynamic model of a shaft torsional and blade bending deformations in rotors, *Computer Methods in Applied Mechanics and Engineering* 169 (1999) 177–190.